A Remotely Based Evaluation of Urban Expansion and its Impact in Land Surface Temperature: A Case Study of Ogbomoso

Article *in* The Journal of Engineering Research [TJER] · September 2020

2 authors:

Makinde E. O.
University of Lagos
42 PUBLICATIONS **241** CITATIONS

SEE PROFILE

Emmanuel Akiode
University of Lagos
1 PUBLICATION **0** CITATIONS

SEE PROFILE

A Remotely Based Evaluation of Urban Expansion and its Impact in Land Surface Temperature: A Case Study of Ogbomoso

E. O. Makinde[1] and E. O. Akiode[2]
Department of Surveying and Geoinformatics, University of Lagos, Lagos, Nigeria
Email addresses: [1]eomakinde@unilag.edu.ng; [2]akifem.emma@gmail.com

ABSTRACT

Land Surface Temperature (LST) is a fundamental environmental parameter affected by land cover change. Over the years, Ogbomoso had experienced a rapid urban expansion has led to the increase of its surface temperature. This paper, therefore, investigates the urban expansion and its impact on land surface temperature (LST) of Ogbomoso in Oyo state of Nigeria, using Land Satellite (Landsat) images from 1991 to 2019. This is with the view of assessing the extent of the land use and land cover (LC) in Ogbomoso and estimating its land surface temperature. The images were subjected to digital Image Processing (DIP) and analysed using ERDAS Imagine 2014 and ArcGIS 10.6 software. Using these spatio-temporal images with their thermal bands, land cover and LST changes, the spatial patterns of LST and LC were derived to examine the response of LST to urban growth. The findings of this study indicate that previously known rural areas such as Agegunle, Imoji, Alapa and part of Ogbomoso South in 1991 have become urbanized by year 2019, hence, an increase in the LST of these areas over time. Built-up areas such Ajegunle, Lautech and Jagun reported high increase in its surface temperature from about 27°C to about 33°c. This result further showed that new growth areas in Ogbomoso had altered the surface thermal environment. This study therefore, provides reasonable evidence of heating up of our environment.

Keywords: Landsat images; Land cover changes; Land surface temperature; Urbanization; Ogbomoso

1.0 INTRODUCTION

Cities produce associate atmosphere that is clearly distinct from their close areas. As population increases, the urban structures alter the surface energy budget (Whitford, Ennos, and Handley, 2001) and modify the vertical profile of various atmospheric properties that introduce additional sources of heat. When visits are made to urban areas, one observes that the climate conditions within the urban atmosphere is considerably distinct from their rural counterparts. Human activities heat up the environment and this has produced pockets of high temperature across urban cities referred to as Urban Heat Islands (UHI). Argüeso *et al. (*2015) reported that urban climate has so attracted sizeable attention from a broad array of researchers within the previous few decades. Published Urban Heat Islands (UHI) research dates back to over 170 years, beginning with Luke Howard's description of London's urban climate accessed by Howard (2007). Also, Landsberg (1981) reported that growing concern about human influence on their environment has resulted in an extraordinary increase in literature on the subject since the 1950s. Field campaigns and modeling efforts have enlightened our understanding about the various factors responsible for UHI development. Generally speaking, the UHI results from a combination of factors that alter the local energy balance. This includes: the thermal and physical properties of construction materials, building geometry, surface roughness, anthropogenic heat sources, and factors contributing to decreased evapotranspiration (Oke, 1982), others are: seasonal climate, daily synoptic conditions, and also the diurnal cycle play key roles in decisive UHI character (Oke, 1982; Arnfield, 2003). As a result, every geographic region contains a distinctive UHI explicit to the circumstances found there.

The UHI can be quantified and predictions made. Previous studies have shown the use of high-

resolution simulations over longer periods to quantify temperature response to urban expansion and climate change (Argüeso *et al.,* 2015). Georgescu *et al.* (2014) reported an estimated contribution to future mean warming from urban structures in the range 1–2°C by the end of the century while El-Fadel *et al.* (2012) reported 1.1–2°C for minimum temperature by 2050. This is one of the environmental parameters affected by land cover change due to its role in the exchange of earth's surface energy, exchange of surface matter, physical and chemical processes within the atmosphere (Xiao *et al.*, 2007; Butuc and Moldovean, 2012; Deng *et al.*, 2018). At the same time, Land Cover (LC) change is a significant factor affecting Land Surface Temperature (LST). This is because the surface characteristics, reflectance and roughness of different land cover types differ markedly thereby affecting in similar ways the LST associated with them. Intense human activities with rapid urbanization worldwide alter rapidly the land cover and thus LST.

Ogbomoso has experienced rapid development and high growth of urbanization in the past decades. These environmental transformations have changed the physical and natural environment of the area, owing in part to LST being an important parameter in many environmental and climate models (Oguz, 2013). Urban encroachment has been obvious in the suburbs and this has transformed the rural environment into a new urban landscape. Ogbomoso is one of the largest cities in Oyo state. With continuing global warming coupled with unrestrained urban sprawl and in-fill, continuous monitoring to generate reliable estimates of land surface temperature and land cover changes are crucial. The result from this will be useful for appropriate management and policy actions at the metropolitan level for the well-being of its residents. This study, therefore, investigated the changes in LST and LC between 1991 and 2019 using remote sensing technology.

2.0 METHODOLOGY
The methodology adopted in this research consists of data acquisition, land cover (LC) extraction, land surface temperature (LST) determination, generation of LST inventory and the relationship with LC.

2.1 Study Area
Ogbomoso is a town located in Oyo State, southwestern Nigeria. It lies on the Plateau of Yorubaland (elevation 1,200 feet [366 m]) in an area of savanna and farmland and at the intersection of roads from Oyo, Ilorin, Oshogbo, and Ikoyi.
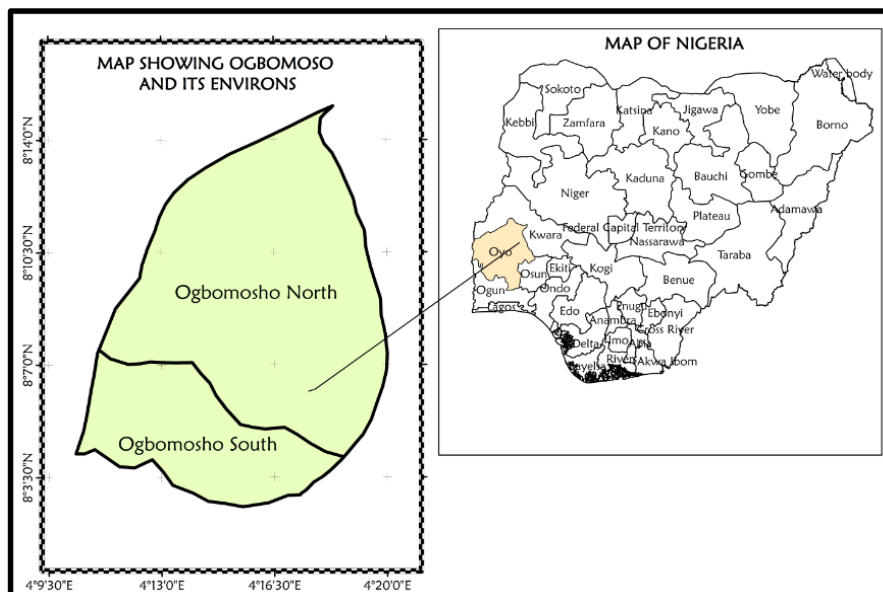
Figure 1. Map of the study Area

2.2 Data acquisition

This study used images from Landsat 5 Thematic Mapper (TM) of 1991, Landsat 7 Enhanced Thematic mapper of 2003, and Landsat 8 Operational Land Imager (OLI) Thermal Infrared Sensor of 2015 and 2019 which were acquired from the United States Geological Surveys (USGS) Global Visualisation online portal - http://glovis.usgs.gov. A gazetteer of town and community locations was also acquired from the National Population Commission (NPopC). To overcome measurement and geometry computation difficulties, all datasets in different formats and projections were harmonized to fit into a uniform coordinate system - WGS84 UTM Zone 31N. Table 1 shows that the Land images were acquired during the dry season for all the years as they fall within December and January and this is a major factor when dealing with temperature.

Table 1: Landsat data-sets used for the land surface temperature determination

Year	Sensor	Scene ID	Path/Row	Date Acquired (mm/dd/yyyy)	Spatial Resolution (m)
1991	TM	LE51910542002355EDC00	191/054	12/27/1991	30.0
2003	ETM+	LE71910542002362EDC00	191/054	01/29/2003	30.0
2015	OLI/TIRS	LE81910542002362EDC00	191/054	12/24/2015	30.0
2019	OLI/TIRS	LE81910542009333ASN00	191/054	1/1/2019	30.0

2.3 Image pre-processing

These images were subjected to digital image processing and the bands stacked. For the layer stacking, the extracted individual bands that make up each of the Landsat scenes acquired were stacked into a single multispectral image using ERDAS Imagine 2014 software. A subset of the Area of Interest (AOI) was extracted and clipped to the administrative boundary shape file (.shp) of Ogbomoso of Oyo state for analysis.

2.4 Land cover classification

The preliminary interpretation of the Landsat images involved categorizing the study area into five land cover classes, namely: bare land, built-up area, wetlands, mixed forests and water bodies. Next, a step-by-step process of training class selection based on the spectral signatures of each class and ancillary data was performed. Care was taken to avoid inclusion of mixed pixels in the training classes to improve the quality of the output classes. Then, supervised classification of the images was performed using the parallelepiped technique. The parallelepiped algorithm is a computationally efficient method of classifying remotely sensed data. It uses a simple decision rule to classify multispectral data. The decision boundaries form an n-dimensional parallelepiped in feature space (Kumar, 2003). If a pixel value lies above the low threshold and below the high threshold for all n bands being classified, it is assigned to the first class matched. If the pixel value falls in multiple classes, it is assigned to the first class matched. Once the supervised classification was performed on each of the Landsat images, they were checked for accuracy using the accuracy assessment tool in ERDAS Imagine while the Google Earth image was the groundtruth data. The feature classes were transferred to ArcGIS 10.6.1 for editing, elimination of spurious clusters and refinement of the output.

2.5 Land surface temperature determination

This study relied on the following thermal bands – TM band 6 and TIRS band 10 for land surface temperature retrieval of Ogbomoso. In order to obtain LST from space radiometry, three main effects need to be considered and corrected for: atmospheric, angular, and emissivity effects. The three major effects of the atmosphere are absorption, upward atmospheric emission, and the downward atmospheric irradiance reflected from the surface (Franca and Cracknell, 1994). LST is based on Planck's function, which relates the radiative energy emitted by a black body (emissivity = 1) to its temperature. However, most natural objects are non-black bodies $(0 < \varepsilon(\lambda) < 1)$, where the spectral emissivity $\varepsilon(\lambda)$ is the ratio between the radiance emitted by an object at wavelength λ and that emitted by a black body at the same temperature. The digital number values on the imagery were converted to radiance, then to at-sensor (top-of-atmosphere) brightness temperature and further, to land surface temperature (LST) in order to draw quantitative analysis from the thermal remote sensing data. The procedure is as follows:

2.4.1 Conversion of digital number to spectral radiance

The LST was retrieved using two major steps: First, the conversion of digital numbers (DNs) of band 6 to Atmospheric radiance (Ar) using equation 1 (Makinde and Agbor, 2019)

$$Ar = \frac{(L_{max}\lambda - L_{min}\lambda)}{Q_{cal}\lambda} * Q_{cal} + L_{min}\lambda \qquad (1)$$

where Ar is the radiance at the sensor ($Wm^{-2}sr^{-1}\mu m^{-1}$), Q_{cal} is the image value (DN), Q_{cal} min represents the minimum DN value corresponding to $L_{min}\lambda$, Q_{cal} max is the maximum pixel value corresponding to $L_{max}\lambda$, $L_{min}\lambda$ is at-sensor radiance scaled to Q_{cal} min in [W/(m²sr: where Q_{cal} min = 1, Q_{cal} max = 255, Q_{cal} = DN and L_{max} and L_{min} are given in the metadata.

To retrieve Ar from Landsat 8 image, the Ugur *et al.* (2016) formula was adopted (equation 2):

$$Ar = mx + a \qquad (2)$$

where m is the multiplicative rescaling factor, x stands for the band 10, and a is the additive rescaling factor.

2.4.2 Conversion of spectral radiance to top-of-atmosphere brightness temperature

After the spectral radiance, $L\lambda$ was computed and the brightness temperature at the satellite level was directly calculated by using the approximation formula as presented in equation 3 (Schott and Volchok 1985).

$$T = \frac{K2}{\log\left(1 + \frac{K1}{L\lambda}\right)} - 273.15 \qquad (3)$$

Where, T is the Top of Atmosphere Brightness Temperature (deg K)
K1 ($Wm^{-2}sr^{-1}\mu m^{-1}$) and K2 (deg K) are pre-launch calibration constants.

Values for $K1$ and $K2$ for Landsat TM and ETM+ are shown in Table 2, while Table 3 shows the values for Landsat 8 TIRS. They are extracted from the downloaded image metadata and these parameters are used for conversion of the spectral radiance to top atmosphere brightness temperature as shown in equation 3.

Table 2: Landsat TM and ETM+ Calibration Constants

	Landsat 5 TM	Landsat 7 ETM+
K1 (Wcm-2sr-1µm-1)	607.76	666.09
K2 (deg K)	1260.56	1282.71

Source: (downloaded image metadata)

Table 3: Landsat 8 (OLI) Calibration Constants

	Band 10	Band 11
K1 (Wcm-2sr-1µm-1)	774.89	480.89
K2 (deg K)	1321.08	1201.14

Source: (downloaded image metadata)

2.4.3 Conversion of Brightness Temperature to Land Surface Temperature

The equation for conversion from brightness temperature to land surface temperature follows Weng *et al.* (2004), Cummings (2007), and Zareie *et al.* (2016). LST was derived from TM 6 and OLI 10 using emissivity corrected model as presented in equation 4.

$$St = \frac{T}{(1 + (\lambda * T/Ar + 1)\, ln\, \varepsilon} \qquad (4)$$

where St = LST, λ = wavelength of emitted radiance (11.345 for TM/ETM+ and 11.5 µm for OLI), ρ = h×c/ (1.438 ×10-2 m K), σ = Boltzman constant (1.38 ×10-23 J/K), h = Planck's constant (6.626×10-34 J s), c = velocity of light (2.998 ×108 m/s), ε = denotes emissivity (Lillesand *et al.*, 2008).

2.5 Determination of points of interest

About nineteen points of interest were selected randomly on the Landsat images of the study area for validation of the Land surface temperature generated using Google Earth Pro. The coordinates of these extracted points were recorded in Excel file format (.csv) and added in a GIS environment.

Using the Extract Values to Point tools and the land surface temperature of each point was generated from 1991 to 2019 and comparison made.

3.0 RESULTS AND DISCUSSION
3.1 Image Classification
Figures 2 and 3 show the multispectral images downloaded after being clipped to the administrative map of Ogbomoso and the classified images respectively. The land cover classes used were built-up area, heavy vegetation, bare land, burnt surfaces and water body, light vegetation for years 1991, 2003, 2015 and 2019.
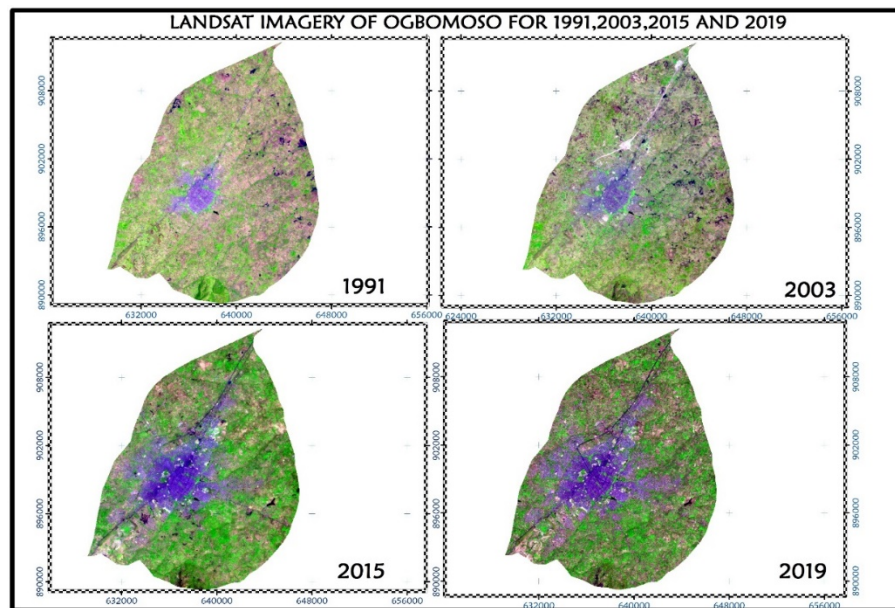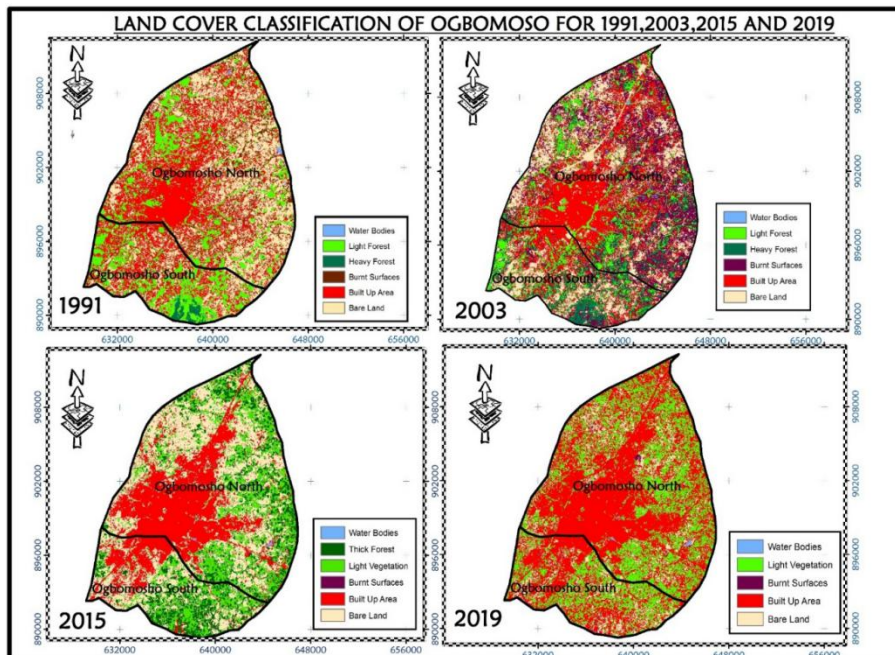

Figure 2: Landsat Imagery Downloaded

Figure 3: The classified images showing the Urban Expansion in red colour

78

Figure 3 shows the gradual urban sprawl from the central part of Ogbomoso and extending to its environs over the years. Table 4 indicates the land use and land cover statistics distribution for the years under consideration. In 1991, bare-land had the highest percentage of 55.26% and decreased to 12.15% by 2019; while built-up area accounted for 20.26% in 1991 but increased to 56.2% by 2019. There was no heavy forest recorded in year 2019. There was no heavy forest recorded in the year 2019. This is as a result of anthropogenic activities which have invaded the heavy forest and reduced it to light forest. The accuracy assessment revealed that the overall classification for year 1991 was 69% and its kappa statistics 0.59, while 2003 was 78% and 0.74 respectively. Years 2015 and 2019 had the same overall accuracy value of 71% and kappa statistics as 0.74 ad 0.70 respectively.

Table 4: Land Use and Land Cover Distribution

Landcover Class	Land use Land Cover Distribution							
	Area (Hec.) 1991	% Classified 1991	Area (Hec.) 2003	% Classified 2003	Area (Hec.) 2015	% Classified 2015	Area (Hec.) 2019	% Classified 2019
Water Bodies	49.77	0.19	54.59	1.51	30.96	0.12	46.71	0.17
Heavy Forest	263.7	0.98	2713.41	10.11	3987.5	14.86	0	0
Burnt Surfaces	1782.27	6.64	5901.75	21.99	38.07	0.14	126.63	0.47
Built Up Area	5437.89	20.26	8425.08	31.39	10131	37.74	15107	56.2
Bare Land	14028.3	52.26	6139.89	22.87	7216	26.88	3266.7	12.15
Light Forest	5279.85	19.67	3607.11	13.44	5437.9	20.26	8334.7	31.01
Total	26841.8	100	26841.8	100	26842	100	26842	100

3.2 Change Detection

The changes in the land cover over a 28-year period in Ogbomoso can be seen in Table 5. Table 5 presents the land cover changes detected between 1991-2003 and 2015-2019. It was observed that there was a change (increase) in the water body from 4.82 hectares in 2003 to 15.75 hectares by 2019. This could be as a result of the clearing of the forest lands to give way to built-up expansion. In line with this, the built-up area increased from 2987.19 hectares in 2003 to 4975.61 hectares by 2019. Burnt surfaces were observed in all the images indicating that forest lands were being cleared regularly. Also, the location of Ladoke Akintola University in Ogbomoso central may have accounted for the vast urban growth in this area.

Table 5: Change Detection

Land Cover Type	1991-2003			2015-2019		
	Area (Hectares)	Area (Hectares)	Change (Hectares)	Area (Hectares)	Area (Hectares)	Change (Hectares)
Water Bodies	49.77	54.59	4.82	30.96	46.71	15.75
Heavy Forest	263.7	2713.41	2449.71	3987.54	0	-3987.54
Burnt Surfaces	1782.27	5901.75	4119.48	38.07	126.63	88.56
Built-Up Area	5437.89	8425.08	2987.19	10131.39	15107	4975.61
Bare Land	14028.3	6139.89	-7888.41	7215.98	3266.72	-3949.26
Light Vegetation	5279.85	3607.11	-1672.74	5437.89	8294.77	2856.88

3.3   Land surface temperature

Figures 4 and 5 show the surface emissivity maps obtained from the conversion of digital number to spectral radiance. Figures 6 and 7 show the land surface temperature map generated from the thermal band of the Landsat imagery of each year. From the map, it can be observed that the temperature increased from the center and stretches out to the northern and southern portion of the study area.
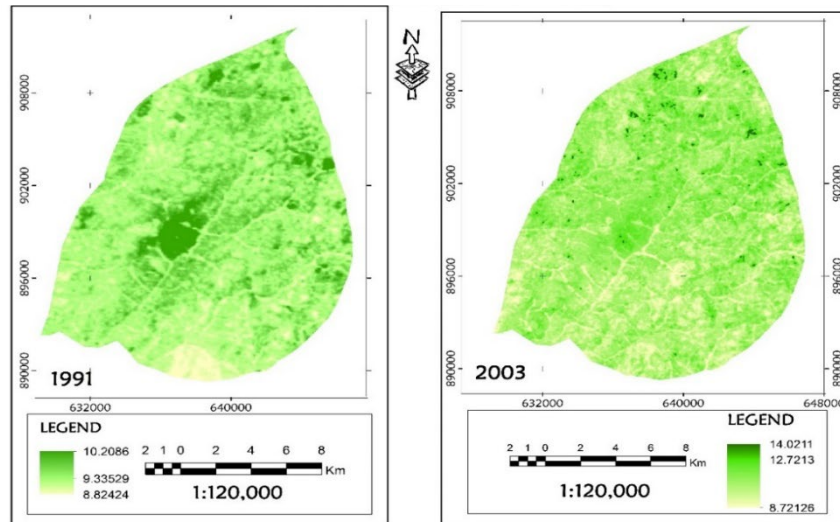

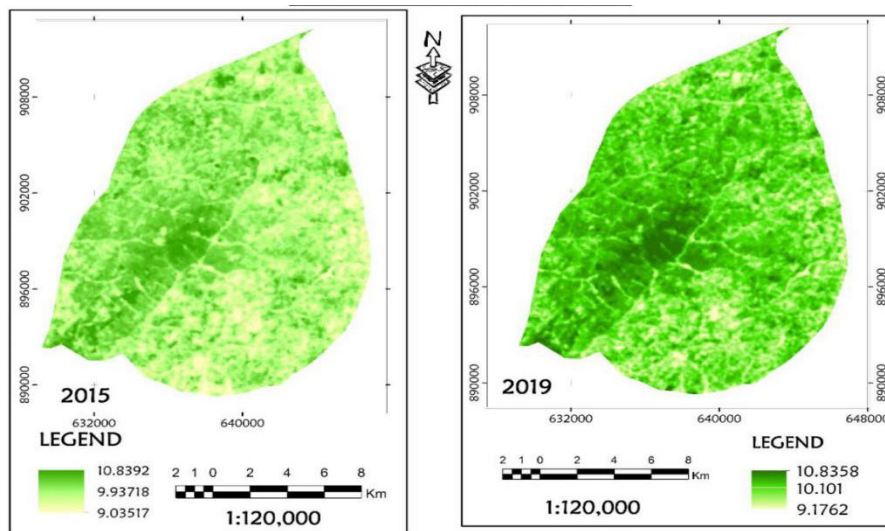**Figure 4: Surface emissivity maps of 1991 and 2003**
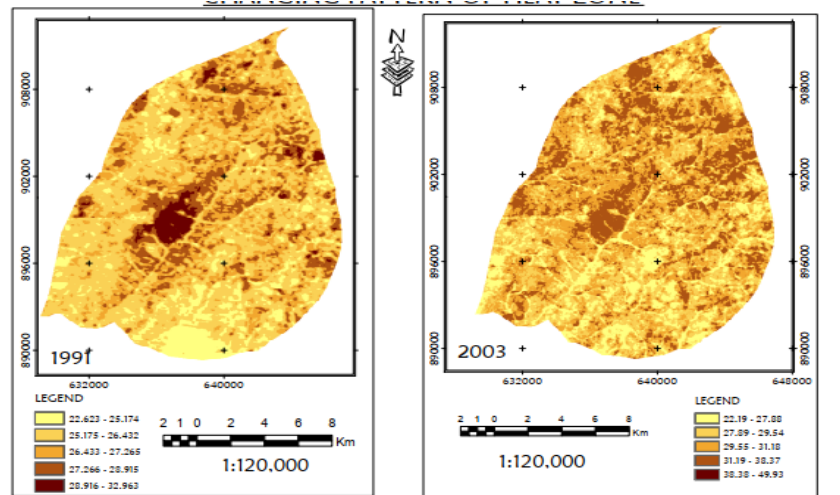

Figure 5: Surface emissivity maps of 2015 and 2019

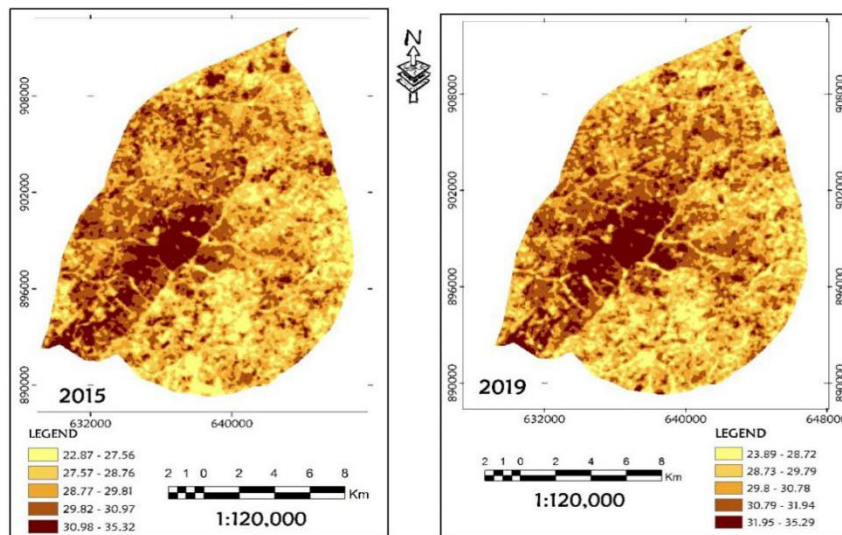**Figure 6. Land surface temperature maps 1991 and 2003**

Figure 7. Land Surface Temperature maps of 2015 and 2019

3.6 Land surface temperature for each selected points of interest

Table 6 affirms that most of the urban areas today were previously ecological assets of forest lands. These forest lands have declined drastically over the years. In 1991, existing built-up areas such as Sabo, Caretake, Ogbomoso Central and Saja had temperature values ranging between 28–31°C, while the average temperature for other wards were between 26–28°C. However, by 2003, the temperature had increased to 30–35°C. This increase in temperature had extended to the surrounding areas such as Imoji, Ajegunle and Under G area. It was observed that the forest lands were set on fire to pave way for construction. This act is evident by the obvious burnt surfaces clearly seen on the images especially in the rural areas. In addition, certain areas such as Ogbomoso Central, Oremerin, and Caretaker recorded a minimum LST change of about 1.0°C in 2003 while other areas such as Orimerin, Jagun, Imoji Ajegunle, Ogbomoso Central had a minimum change in land surface temperature of 0.6°C in 2019.

Table 6: Land surface temperature for selected points of interest

Northing (m)	Easting (m)	Point of Interest	1991-2003			2015-2019		
			LST 1991	LST 2003	Change	2015	2019	Change
643173.23	902967.8	Imoji	28.09	31.73	3.64	30.53	31.17	0.64
636437.17	901103.8	Sabo	26.43	29.54	3.11	29.30	29.55	0.24
637706.74	899293	Ogbomoso	28.92	29.82	0.9	30.44	32.05	1.62
635540.5	900840.5	Olugbon	27.26	30.64	3.37	30.57	31.75	1.17
638008.07	899059.1	Saja	29.33	31.18	1.86	30.75	32.17	1.42
636329.52	897293.2	Arowomole	27.26	30.09	2.83	30.59	32.33	1.74
638001.63	902432.5	Temidire	27.26	31.46	4.19	30.00	31.83	1.83
635243.49	897785.9	Ayegun	28.92	31.18	2.27	31.67	33.13	1.46
633902.14	897807.4	Ibapon	26.01	29.82	3.8	30.54	31.87	1.33
635639.28	898488.4	Caretaker	30.14	31.46	1.32	31.77	33.01	1.24
635995.72	898221.6	Oremerin	28.92	30.36	1.45	31.57	32.47	0.9
638100.21	901446.5	Lautech	28.09	31.18	3.09	30.58	31.84	1.26
639536.57	901980.7	Under-G Area	27.68	32.27	4.59	30.96	32.15	1.19
641411.19	891888.2	Jagun	26.43	28.99	2.56	27.98	28.75	0.76
634028.19	902938.9	Ajegunle	27.68	32.81	5.13	29.63	30.40	0.77
634692.12	841112.2	Alapa	27.26	29.54	2.28	30.29	31.85	1.56

4.0 CONCLUSION

This study assessed the urban expansion of Ogbomoso and its impact on the land surface temperature. For the past 28 years, Ogbomoso and its environs have undergone dramatic changes in its land surface characteristics. Increase in population, the demand for sustenance and infrastructural development have been contributory factors to these changes. Landsat thermal band data were used to extract surface temperatures for 1991, 2003, 2015, and 2019. It was observed from the retrieved temperature data that areas of higher human habitation (more built-up) have higher temperature than surrounding areas. These areas were regions that had developed into urban settings owing to population increase. Thus, areas of higher urban expansion had higher temperature ratings from 27° to 33° between 1991 and 2019. This study established that the areas of increased LST coincided directly with areas of rapid increase in built-up. The increase in the land surface temperature over the decades further points to a warming surface temperature across the city. From this, we could infer the relationship between the Land Cover Type and the Land Surface Temperature.

REFERENCES

Arnfield, A. J. (2003). Two decades of urban climate research: a review of turbulence, exchanges of energy and water, and the urban heat island. *International Journal of Climatology: A Journal of the Royal Meteorological Society*, 23(1), 1-26.

Argüeso, D., Evans, J. P., Pitman, A. J., Di Luca, A. (2015). Effects of city expansion on heat stress under climate change conditions. *PLoS one, 10*(2), e0117066.

Butuc, B. R. and Moldovean, G., (2011). Environmental impact scenario of an azimuthal tracked PV platform based on CO2emissions reduction. *Environmental Engineering and Management*, 10, 271-276.

Cummings, S. (2007). An Analysis of Surface Temperature in San Antonio, Texas. Term Project. EES5053/ES4093: *Remote Sensing*, UTSA.

Deng, Y., Wang, S., Bai, X., Tian, Y., Wu, L., Xiao, J., Chen, F. and Qian, Q. (2018). Relationship among land surface temperature and LUCC, NDVI in typical karst area. *Scientific reports,* 8(1), 1-12.

El-Fadel, M., Ghanimeh, S., Maroun, R., and Alameddine, I. (2012). Climate change and temperature rise: Implications on food-and water-borne diseases. *Science of the Total Environment, 437*, 15-21.

Franc, G. B., and Cracknell, A. P. (1994). Retrieval of land and sea surface temperature using NOAA-11 AVHRR· data in north-eastern Brazil. *International Journal of Remote Sensing*, 15(8), 1695-1712.

Georgescu, M., Morefield, P. E., Bierwagen, B. G., and Weaver, C. P. (2014). Urban adaptation can roll back warming of emerging megapolitan regions. *Proceedings of the National Academy of Sciences, 111*(8), 2909-2914.

Howard, L. (2007). The Climate of London. IAUC edition available at www.lulu.com in two volumes.

Kumar, K. S., Bhaskar, P. U., and Padmakumari, K. (2012). Estimation of land surface temperature to study urban heat island effect using Landsat ETM+ image. *International journal of Engineering Science and technology, 4*(2), 771-778.

Landsberg, H. (1981). *The Urban Climate*. 1st Edition, Volume 28, ISBN: 9780124359604, Academic Press

Lillesand, T., Kiefer, R. and Chipman, J. (2004). *Remote sensing and image interpretation*. Chichester: John Wiley.

Makinde, E., & Agbor, C. (2019). Geoinformatic assessment of urban heat island and land use/cover processes: a case study from Akure. *Environmental Earth Sciences, 78*(15), 483.

Oguz, H. (2013). LST Calculator: a program for retrieving land surface temperature from Landsat TM/ETM+ imagery. *Environmental Engineering and Management*,12(3), 549 –555

Oke, T. R. (1982). The energetic basis of the urban heat island. Q J. R. *Meteorol. Soc.*108, 1–24.

Schott, J. R. and Volchok W. J. (1985). Thematic Mapper thermal infrared calibration, *Photogramm. Eng. Remote Sensing,* 51, 1351-1357

Ugur, S., Sarıışık, M., Türkoğlu, G., Erkan, G. and Erden, E. (2016), Layer by layer assembly of antibacterial inclusion complexes, *International Journal of Clothing Science and Technology*, 28(3), 368-377. https://doi.org/10.1108/IJCST-03-2016-0032

Weng, Q., Lu, D., and Schubring, J. (2004). Estimation of land surface temperature –vegetation abundance relationship for urban heat island studies. *Remote Sensing of Environment*, 89(4), 467 –483.

Whitford, V., Victoria, E., and Handley, J. F. (2001). "City form and natural process" - Indicators for the ecological performance of urban areas and their application to Merseyside, UK. *Landscape and Urban Planning*. 57, 91-103. https://doi.org/10.1016/S0169-2046(01)00192-X.

Xiao, R., Ouyang, Z., Zheng, H., Li, W., Schienke, E., and Wang, X. (2007). Spatial pattern of impervious surfaces and their impacts on land surface temperature in Beijing, China. *Journal of environmental sciences* (China). 19(2), 250-256. https://doi.org/10.1016/S1001-0742(07)60041-2.

Zareie, S., Khosravi, H., and Nasiri, A. (2016). Derivation of Land Surface Temperature from Landsat Thematic Mapper (TM) sensor data and analysing relation between Land Use changes and Surface Temperature. *Solid Earth. Discuss*. 1-15.